

Illumination compensation using Poynting vectors, with special treatment for multiples

Alan Richardson* and Alison E. Malcolm, Department of Earth, Atmospheric and Planetary Sciences, Massachusetts Institute of Technology

SUMMARY

We describe a method for compensating Reverse Time Migration seismic images for illumination effects using Poynting vectors. This scheme allows internal multiples to be used more effectively, by appropriately boosting their image contribution amplitude, attenuating certain types of image artifacts caused by their inclusion, and ensuring that they add constructively to the image. It also has benefits for imaging with overturned waves. We demonstrate the method with a synthetic model, yielding improved results compared to standard Reverse Time Migration.

INTRODUCTION

Seismic imaging attempts to construct an image of subsurface structure. Migration methods such as Reverse Time Migration (RTM, Baysal et al. (1983)) seek to achieve this by positioning reflected energy at the locations of the reflectors. Although it has been shown that under idealized conditions the amplitudes in images produced with RTM are directly related to the reflector properties (Chattopadhyay and McMechan, 2008), in general the amplitudes are also significantly affected by other factors. One of these is uneven illumination. The effect of this is that reflectors in poorly illuminated areas, such as at the edge of surveys or below salt, will have lower amplitude than better illuminated structures with similar reflectivity.

Many attempts have been made to compensate for illumination effects in seismic images. Several of these methods are preconditioners for Least-Squares Migration (LSM, Nemeth et al. (1999)), which is unsurprising given LSM's goal of producing true amplitude images. Early attempts, such as Rickett (2003), use a single scaling factor for each image point. The image amplitude is divided by the scaling factor (a measure of illumination) at each point in an attempt to remove illumination effects from the image. While this may reduce the impact of illumination variations across the image, illumination depends not only on location, but also on reflector dip. It may not be possible to illuminate a flat reflector at the edge of a survey, while an inclined reflector at the same location may be well illuminated. Most recent proposals have therefore sought to determine image amplitude and illumination as functions of position and angle. The approaches are often differentiated by the proposed means of extracting the angular dependence of the image and illumination. Several methods employ forms of wavelets (Herrmann et al., 2009; Mao et al., 2010), others exploit the pseudodifferential nature of the illumination compensation operator (Nammour and Symes, 2009; Demanet et al., 2012). Cao and Wu (2009) propose the use of local slant stacks, and Cao (2013) uses a local transformation of point spread functions to obtain the angular information.

In this paper we examine the use of Poynting vectors to extract angular information necessary for illumination compensation. We place particular emphasis on correctly incorporating the information provided by multiples, overturned waves, and other phenomena that can cause an interface to be imaged from below. This is achieved in several steps. We first use Poynting vectors to bin, by propagation direction, wavefields created by injecting wavelets at source and receiver locations. At source locations we inject the source wavelet used in the seismic experiment, while at receiver locations we inject a unit pulse, creating an approximation of the Green's functions from these positions. This is used to determine the source and receiver illumination of each shot. From these quantities we calculate the acquisition dip response (ADR), which expresses the illumination of a reflector at a particular point and dip angle. We again use Poynting vectors to bin the source and receiver (data) wavefields by propagation angle when constructing the image. These angles are used to infer the reflector dip in the image. The image is compensated for illumination with a division by ADR. Measures of uncertainty are then derived, such as the standard deviation of the compensated images over shots, weighted by ADR.

Poynting vectors

Poynting vectors are enjoying a surge of interest from the seismic imaging community. Applications thus far have focused on their use in reducing low frequency artifacts in images (Yoon and Marfurt, 2006), obliquity corrections (Costa et al., 2009), and the construction of angle gathers (Dickens and Winbow, 2011). An important advantage of the Poynting vector approach to determining wave propagation direction is its efficient computation. It does suffer from some problems, however, in particular its difficulty distinguishing overlapping wavefronts, and the lack of stability in output. Additional difficulties are discussed in Patrikeeva and Sava (2013). Several recent proposals attempt to mitigate these issues (Tang et al., 2013; Yan and Ross, 2013).

Multiples

Internal multiples (waves reflected multiple times in the subsurface) have long been of interest in seismic imaging. As migration methods generally linearize the problem of positioning reflectors by making the single scattering assumption (Bleistein et al., 2001), multiples are often seen as noise that must be removed (Weglein et al., 1997). The tantalizing prospect of exploiting the useful information contained in multiples has led others to propose schemes for imaging with multiples (Malcolm et al., 2009; Fleury, 2013).

Cao and Wu (2009) show that internal multiples can provide more even illumination in subsalt areas than singly-scattered primaries. There are also several additional motivations for combining the inclusion of multiples with an illumination compensation method such as the one we propose. One is that multiples are usually significantly weaker than primaries, and

Illumination compensation with Poynting vectors

so illumination compensation is necessary in order for them to contribute substantially to the image. A second reason is to reduce artifacts caused by the inclusion of multiples. Multiples can be automatically used for imaging in RTM by including discontinuities in the migration velocity model at the locations of multiple generating reflectors. Doing so can introduce artifacts in the image. If we can illuminate these artifacts with other wavepaths that do not also produce an artifact there, then the illumination of the artifact will be increased without increasing the image amplitude. This will reduce the amplitude of the artifact in the illumination compensated image.

Although calculating propagation directions to perform illumination compensation increases the computational cost compared to regular RTM, the availability of this information provides a third reason for using such a scheme when incorporating multiples. Internal multiples may reflect from the opposite side of an interface to primaries. Richardson and Malcolm (2013) demonstrate that since this results in a reflection coefficient for internal multiples with the opposite sign to that for primaries, without additional care, multiples may actually subtract from the image rather than adding to it. The same situation can also occur with overturned waves (Biondi and Shan, 2002). Using the propagation direction information calculated during an illumination compensation method, we can detect when an interface is being imaged from “below” and reverse the sign of the contributed image amplitude so that the contribution adds constructively.

Uncertainty

While illumination compensation can improve images by removing the effect of certain acquisition and subsurface structures that can impair amplitude accuracy, it may also enhance unwanted artifacts. An artifact in a poorly illuminated area of the subsurface may have its amplitude boosted so that it has similar prominence in the image to well illuminated reflectors. To contend with this, we complement the images with a measure of uncertainty.

METHOD

In order to produce an illumination compensated image we need uncompensated images, and illumination, both binned by reflector dip.

Uncompensated images

Before illumination compensation, the images we create are similar to regular RTM images, binned by apparent reflector dip. They can therefore be produced by augmenting a regular RTM method with a Poynting vector calculation step to determine wave propagation directions.

We calculate Poynting vectors of the source and receiver wavefields during migration using the method described in Yoon and Marfurt (2006). We use these Poynting vectors to determine the reflector dip angle, θ , via.

$$\theta = \mathbf{VA}(\hat{\alpha}_s + \hat{\alpha}_r), \quad (1)$$

where $\hat{\alpha}_s$ and $\hat{\alpha}_r$ are the normalized Poynting vectors of the source and receiver (data) wavefields, respectively. The direction of source wave is computed for time going forwards, while the receiver wave direction is computed with time going backwards. The operator \mathbf{VA} converts a vector to its angle (in the range $[0, 2\pi)$ radians) from horizontal. For simplicity we will work in 2D; extension to 3D is straightforward.

Any of the standard RTM imaging conditions can be used; we apply the zero lag cross-correlation condition (Claerbout, 1971). To enhance the image we augment this with two additional filters. The first is to reverse the sign of image contributions arising from wavepaths that reflect on the underside of reflectors. This is accomplished by multiplying the image contribution by -1 if $\theta > \pi$. The second is the reflection angle taper described by Costa et al. (2009). This uses the Poynting vectors that we have calculated to determine the scattering angle, and then reduces the amplitude of contributions due to high scattering angles (which are likely to be artifacts caused by direct arrivals, or reflections from sharp changes in the velocity model). In our notation, the scattering angle (ϕ) is calculated with quantities already available, using

$$\cos^2 \phi = \frac{1}{2} \left(1 + \frac{\alpha_s \cdot \alpha_r}{\|\alpha_s\| \|\alpha_r\|} \right). \quad (2)$$

Finally, we use the modulo operation to fold θ into the range $[0, \pi)$. This is done so that a reflector imaged from above is identified with the same reflector imaged from below. The image contribution is then added to the relevant bin corresponding to θ . Upon completion, we have an image binned by apparent reflector dip.

Illumination

In order to determine how well a reflector of a particular dip at a given point in the subsurface is illuminated (which, following the lead of others, we refer to as the “acquisition dip response”), we need to know how the image relates to the actual reflectivity. For our chosen imaging condition, after making several approximations and assuming good receiver coverage, we deduce

$$Im_s(\mathbf{x}, \theta) \propto m(\mathbf{x}, \theta) \int_0^T dt_1 u(\mathbf{x}, \mathbf{x}_s, t_1, \alpha_s) \frac{\partial^2 u(\mathbf{x}, \mathbf{x}_s, t_1, \alpha_s)}{\partial t_1^2} \times \sum_{\mathbf{x}_r \in x_r} \int_0^T dt_2 G^2(\mathbf{x}, \mathbf{x}_r, t_2, \alpha_r), \quad (3)$$

where $Im_s(\mathbf{x}, \theta)$ is the uncompensated image at position \mathbf{x} produced by shot s , for a reflector of amplitude m with dip θ . T is the recording time, $u(\mathbf{x}, \mathbf{x}_s, t_1, \alpha_s)$ is the component of the source wave propagating in direction α_s at the given position and time, x_s is the set of receiver locations for the shot s , and $G(\mathbf{x}, \mathbf{x}_r, t_2, \alpha_r)$ is the Green’s function from the receiver location \mathbf{x}_r , arriving at \mathbf{x} with propagation direction α_r .

This prompts the definition of two new quantities. The source illumination,

$$Illum_s^{src}(\mathbf{x}, \alpha_s) = \int_0^T dt_1 u(\mathbf{x}, \mathbf{x}_s, t_1, \alpha_s) \frac{\partial^2 u(\mathbf{x}, \mathbf{x}_s, t_1, \alpha_s)}{\partial t_1^2}, \quad (4)$$

Illumination compensation with Poynting vectors

can be calculated by forward propagating the source wave u , and accumulating over time at each location the product of this wave with its second time derivative, binned by propagation direction α_s . The directional binning is achieved by using Poynting vectors. Receiver illumination for receiver r ,

$$Illum_{s,r}^{rcv}(\mathbf{x}, \alpha_r) = \int_0^T dt_2 G^2(\mathbf{x}, \mathbf{x}_r, t_2, \alpha_r), \quad (5)$$

is calculated by propagating a unit impulse from the receiver location, to approximate the Green's function (with higher accuracy when smaller time step sizes are used). The square of this Green's function, binned by propagation direction α_r , is accumulated over time. We then need to sum the illuminations of each receiver location in the shot to obtain its total receiver illumination:

$$Illum_s^{rcv}(\mathbf{x}, \alpha_r) = \sum_{\mathbf{x}_r \in \mathcal{X}_r} Illum_{s,r}^{rcv}(\mathbf{x}, \alpha_r). \quad (6)$$

Acquisition dip response

The ADR for a shot is given by the product of the source and receiver illuminations. Unlike those quantities, which are binned by propagation direction, ADR depends on reflector dip. We therefore need to convert using the same relations as described above for the uncompensated images. A shot's ADR is then

$$ADR_s(\mathbf{x}, \theta) = \sum_{\phi} Illum_s^{src}(\mathbf{x}, \alpha_s) Illum_s^{rcv}(\mathbf{x}, \alpha_r), \quad (7)$$

where the scattering angle, ϕ is as defined in Eq. 2.

Illumination compensation

To remove the effect of illumination on the image, we divide the uncompensated image by the ADR. The compensated illumination for a single shot is therefore:

$$Im_s^c(\mathbf{x}, \theta) = \frac{Im_s(\mathbf{x}, \theta)}{ADR_s(\mathbf{x}, \theta)} \quad (8)$$

The robustness of regular RTM is significantly enhanced by stacking the output images from different shots. We wish to obtain the same benefit, however merely stacking the compensated images from each shot would not incorporate information about illumination: the amplitude at a point from a shot that illuminates that point poorly would be given equal weight to a shot that illuminates it well. To account for this, we instead stack by calculating the mean weighted by ADR. The stacked image is therefore:

$$Im^c(\mathbf{x}, \theta) = \frac{\sum_{\mathbf{x}_s} \frac{Im_s(\mathbf{x}, \theta)}{ADR_s(\mathbf{x}, \theta)} ADR_s(\mathbf{x}, \theta)}{\sum_{\mathbf{x}_s} ADR_s(\mathbf{x}, \theta)} = \frac{\sum_{\mathbf{x}_s} Im_s(\mathbf{x}, \theta)}{\sum_{\mathbf{x}_s} ADR_s(\mathbf{x}, \theta)} \quad (9)$$

Uncertainty

Regular RTM conveys uncertainty in images by reducing amplitude. Poorly illuminated areas, or areas where different shots do not stack coherently, have low amplitude. This uncertainty is, however, mixed with the effect of reflectivity. It is not clear

whether a location in the image has low amplitude because of low reflectivity, or because of one of the measures of uncertainty: low illumination or lack of agreement among shots. To clarify the uncertainty in images, we propose complementing compensated images with images of ADR and a measure of coherence between shots. For the latter, one possibility is to compute the standard deviation of $Im_s^c(\mathbf{x}, \theta)$ with respect to s (shot), weighted by ADR. This expresses the lack of consistency between shots, with a small number indicating a small spread in amplitude between shots. Some spread is expected, since different shots will produce waves that reflect from a point at different angles, experiencing different coefficients of reflection. This could be reduced by attempting to approximately compensate for scattering angle. Algorithms such as that proposed by West (1979) allow the standard deviation to be computed in a single pass, which means that shots can be added to it as they are calculated, and so images from all of the shots do not need to be stored.

RESULTS

To test illumination compensation using Poynting vectors, including the special treatment of multiples that we described, we consider the simple model shown in Fig. 1. We use source and receivers in a line at the surface, with the same receiver locations used for all shots. There are no paths that allow primaries to return to the surface receivers after reflecting from the vertical interface, and so this feature can only be imaged using multiples. We assume that we know the location of the lower horizontal reflector, and have included this in the migration velocity model, but the upper horizontal reflector and vertical reflector are replaced by the constant background velocity in the migration model.

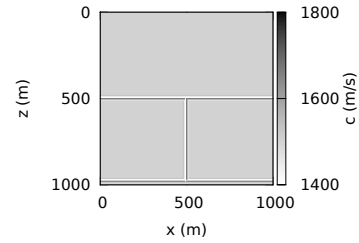


Figure 1: Model consisting of two horizontal reflectors and one vertical reflector connecting them.

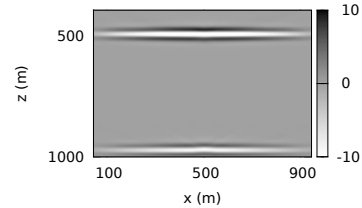


Figure 2: The image produced by regular RTM.

Illumination compensation with Poynting vectors

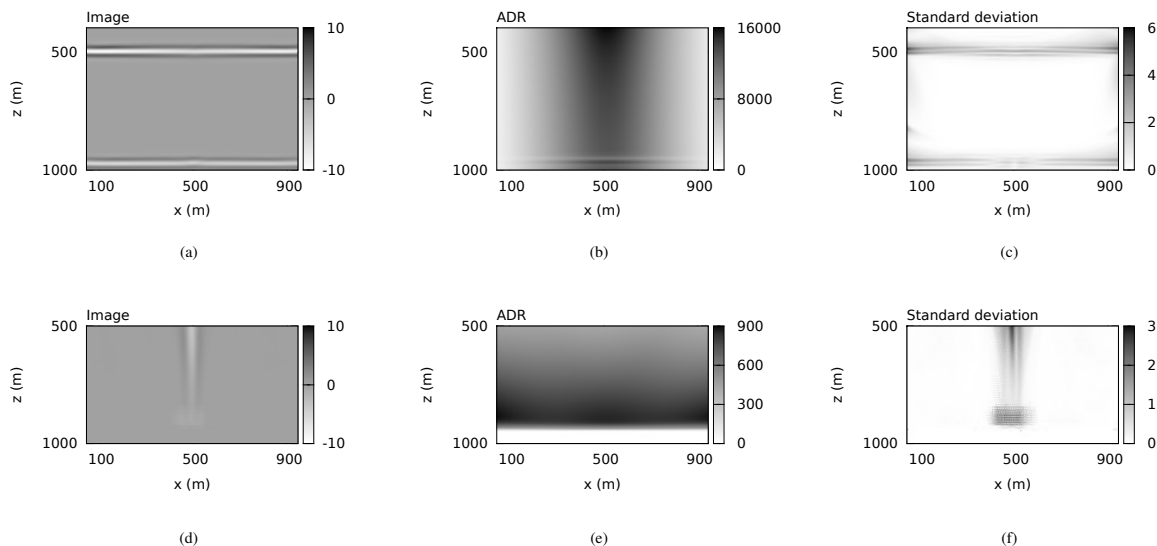


Figure 3: The output of the illumination compensating method. Top: horizontal reflector dip. Bottom: vertical reflector dip.

The image produced by regular RTM with a zero lag cross-correlation imaging condition and scattering angle filter is shown in Fig. 2. Although it images both of the horizontal reflectors, the imprint of illumination is clearly visible in the decreasing amplitude towards the edges of the survey area. The vertical reflector is not visible. Because the bottom reflector was included in the model, multiples will have been generated from this interface, but their amplitude is too small compared to the primaries for their contributions to be visible. Furthermore, without reversing the sign of contributions from different sides of the interface (multiples incident on the left and right sides of the reflector), the reflector amplitudes imaged with multiples will not stack constructively.

We present the images produced with the illumination compensation method by reflector dip in Fig. 3. To convey uncertainty, the ADR and standard deviation of compensated image amplitude over shots, weighted by ADR, are also shown. The image for horizontal reflectors is noticeably improved from the regular RTM case, with the reflector amplitude being almost constant along the interfaces.

In the model, both horizontal reflectors have the same amplitude oscillation, and therefore have the same reflectivity. Neither the regular RTM image nor the illumination compensated image have equal amplitude for these two reflectors, however. One cause for this is transmission losses. The upper reflector causes part of the energy reflected from the lower reflector to be reflected back into the subsurface, so only part of the reflected energy is recorded by the receivers (Richardson and Malcolm, 2013). This is not accounted for by RTM, even when performing illumination compensation. A second cause is that the lower reflector is further from the sources and so is less well illuminated. This effect is corrected by illuminated compensation, which results in the relative amplitude difference between the peak amplitudes of the horizontal reflectors being 9% smaller in the illumination compensated case.

For vertical reflectors, the ADR is zero below the lower reflector. This is because we rely on multiples produced by the lower reflector to image vertical reflectors, and so we are not able to illuminate any below the bottom reflector.

CONCLUSION

Poynting vectors provide an efficient means of extracting wave propagation direction, which we use to bin image amplitude by apparent reflector dip, and determine the illumination for each position and reflector dip (acquisition dip response). This enables us to separate illumination effects from the image, producing more easily interpretable results. To convey uncertainty in the image we propose also presenting ADR and standard deviation images. With special treatment for waves incident from different sides of an interface, we are able to use multiples to add constructively to the image, imaging structures, such as vertical fractures, that present difficulties when using primaries alone.

ACKNOWLEDGMENTS

The authors wish to thank Total for support, and Paul Williamson of Total for his input.

Illumination compensation with Poynting vectors

REFERENCES

- Baysal, E., D. Kosloff, and J. Sherwood, 1983, Reverse time migration: *Geophysics*, **48**, 1514–1524.
- Biondi, B., and G. Shan, 2002, Prestack imaging of overturned reflections by reverse time migration: SEG Technical Program Expanded Abstracts 2002, 1284–1287.
- Bleistein, N., J. Cohen, and J. Stockwell, 2001, *Mathematics of multidimensional seismic imaging, migration, and inversion*: Springer. Interdisciplinary Applied Mathematics.
- Cao, J., 2013, Resolution/illumination analysis and imaging compensation in 3D dip-azimuth domain: SEG Technical Program Expanded Abstracts 2013, Society of Exploration Geophysicists, 3931–3936.
- Cao, J., and R. Wu, 2009, Full-wave directional illumination analysis in the frequency domain: *Geophysics*, **74**, S85–S93.
- Chattopadhyay, S., and G. McMechan, 2008, Imaging conditions for prestack reverse-time migration: *Geophysics*, **73**, S81–S89.
- Claerbout, J., 1971, Toward a unified theory of reflector mapping: *Geophysics*, **36**, 467–481.
- Costa, J., F. Silva Neto, M. Alcántara, J. Schleicher, and A. Novais, 2009, Obliquity-correction imaging condition for reverse time migration: *Geophysics*, **74**, S57–S66.
- Demagnet, L., P.-D. Létourneau, N. Boumal, H. Calandra, J. Chiu, and S. Snelson, 2012, Matrix probing: A randomized preconditioner for the wave-equation hessian: *Applied and Computational Harmonic Analysis*, **32**, 155–168.
- Dickens, T., and G. Winbow, 2011, RTM angle gathers using Poynting vectors: SEG Technical Program Expanded Abstracts 2011, 3109–3113.
- Fleury, C., 2013, Increasing illumination and sensitivity of reverse-time migration with internal multiples: *Geophysical Prospecting*, **61**, 891–906.
- Herrmann, F. J., C. R. Brown, Y. A. Erlangga, and P. P. Moghadam, 2009, Curvelet-based migration preconditioning and scaling: *Geophysics*, **74**, A41–A46.
- Malcolm, A. E., B. Ursin, and M. V. de Hoop, 2009, Seismic imaging and illumination with internal multiples: *Geophysical Journal International*, **176**, 847–864.
- Mao, J., R.-S. Wu, and J.-H. Gao, 2010, Directional illumination analysis using the local exponential frame: *Geophysics*, **75**, S163–S174.
- Nammour, R., and W. Symes, 2009, Approximate constant density acoustic inverse scattering using dip-dependent scaling: SEG Technical Program Expanded Abstracts 2009, Society of Exploration Geophysicists, 2347–2351.
- Nemeth, T., C. Wu, and G. T. Schuster, 1999, Least-squares migration of incomplete reflection data: *Geophysics*, **64**, 208–221.
- Patrikeeva, N., and P. Sava, 2013, Comparison of angle decomposition methods for wave-equation migration: SEG Technical Program Expanded Abstracts 2013, 3773–3778.
- Richardson, A., and A. Malcolm, 2013, Reverse time migration in the presence of known sharp interfaces: SEG Technical Program Expanded Abstracts 2013, 3974–3978.
- Rickett, J. E., 2003, Illumination-based normalization for wave-equation depth migration: *Geophysics*, **68**, 1371–1379.
- Tang, C., D. Wang, and H. Jiang, 2013, RTM angle gathers with Gaussian weighted time-lapse Poynting vectors and receiver wavefield reconstruction in forward time direction: SEG Technical Program Expanded Abstracts 2013, 3779–3783.
- Weglein, A., F. Gasparotto, P. Carvalho, and R. Stolt, 1997, An inverse-scattering series method for attenuating multiples in seismic reflection data: *Geophysics*, **62**, 1975–1989.
- West, D. H. D., 1979, Updating mean and variance estimates: An improved method: *Commun. ACM*, **22**, 532–535.
- Yan, J., and W. Ross, 2013, Improving the stability of angle gather computation using Poynting vectors: SEG Technical Program Expanded Abstracts 2013, 3784–3788.
- Yoon, K., and K. Marfurt, 2006, Reverse-time migration using the Poynting vector: *Exploration Geophysics*, **37**, 102–107.